Clays and Clay Minerals, Vol. 47, No. 4, 505–514, 1999.

PEDOGENIC FORMATION OF KAOLINITE-SMECTITE MIXED LAYERS IN A SOIL TOPOSEQUENCE DEVELOPED FROM BASALTIC PARENT MATERIAL IN SARDINIA (ITALY)

DOMINIQUE RIGHI,[1] FABIO TERRIBILE,[2] AND SABINE PETIT[1]

[1] UMR-CNRS 6532 "Hydrogéologie, Argiles, Sols et Altérations" Faculté des Sciences, 86022 Poitiers Cedex, France
[2] CNR-ISPAIM, PO Box 101, 80040 San Sebastiano al Vesuvio, Napoli, Italy

Abstract—Formation of kaolinite-smectite (K-S) mixed layers in a soil toposequence developed from basaltic parent material was examined. The soil formed in a temperate climate with alternating dry and wet seasons in Sardinia (Italy). Chemical composition and charge characteristics of the smectite component in the K-S mixed layers were analyzed to help determine a mechanism for formation. Soils were sampled at the top, intermediate, and base of a steep (35%) slope. As indicated by X-ray diffraction data, the fine clay fraction (<0.1 μm) in the soils is dominated by K-S with a decreasing proportion of kaolinite from the top (70%) to the base (30%). Rapid internal drainage induced by the slope is probably the major factor responsible for the formation of K-S. Chemical composition and charge characteristics of the smectite component in the K-S were analyzed by X-ray diffraction (intercalation with alkylammonium ions), cation exchanged capacity (CEC) and surface area measurements, and infrared spectroscopy. Results indicate that the smectite component is nearly identical over the soil toposequence. The smectite component is the same with respect to charge magnitude and chemical composition, independent of the proportion of kaolinite and smectite components. This suggests the pedogenic formation of K-S by transformation of smectite through dissolution of some smectite layers and subsequent crystallization of kaolinite between the layers of the remaining smectite crystallites.

Key Words—Basaltic Rock (Weathering), Kaolinite-Smectite Mixed Layers, Sardinia, Smectite-Layer Charge, Soils.

INTRODUCTION

Interstratification of 1:1 and 2:1-type layer silicates is not widely reported, although such minerals in soils may be more common than is currently appreciated (Wilson, 1987). Pedogenic formation of kaolinite-smectite (K-S) mixed layers was described in tropical and subtropical areas, primarily in the "red-black" soil sequences (Kantor and Schwertmann, 1974; Herbillon *et al.*, 1981; Yerima *et al.*, 1985). In temperate areas K-S mixed layers were reported but they are probably inherited from the parent rock (Wilson and Cradwick, 1972) or associated with polygenetic soil profiles (Jaynes *et al.*, 1989). According to Hughes *et al.* (1993), the conditions under which K-S mixed layers appear to form by pedogenesis include the presence of: 1) 2:1 clay mineral parent materials rich in alumina and iron, 2) a humid to subarid climate, 3) plants capable of extracting silica, 4) sufficient time, and 5) drainage. They also concluded that the mechanism of formation of K-S mixed layers is poorly understood. Dissolution-recrystallization processes or "stripping" of the tetrahedral sheet of a preexisting 2:1 layer phyllosilicate are possible mechanisms. In addition, Srodon (1980) suggested that K-S mixed layers form from smectite by the dissolution of some layers and subsequent crystallization of kaolinite in the interlayer of the remaining smectite.

The objective of this paper is to report the occurrence of pedogenic K-S mixed layers with different proportions of kaolinite, in a soil toposequence developed from basaltic parent material, under a mediterranean climate. The chemistry of soil solutions is believed to change over the toposequence. Chemical composition and charge characteristics of the smectite component in the K-S mixed layers were analyzed to help determine why these materials form. We conclude that K-S formed through dissolution of some preexisting smectite layers because the smectite component in the K-S has a constant crystal chemistry.

MATERIALS AND METHODS

Soil toposequence

The study site is located in Sardinia, Italy, near the village Guspini (Oristano) at Serra Pubusa. The landscape consists of eroded hills developed from basaltic rocks and grading into an alluvial plain. At the study site, the alluvial plain catchment extends only on the basaltic rock formation. The toposequence was selected on the slope of an isolated hill. The hill has an altitude of 130 m above sea level and grades with a mean slope gradient of 15% onto the alluvial plain, which is ~50 m altitude. Three soils, located at the summit, midslope, and at the footslope on the alluvial plain, were described and sampled (Figure 1). The soils are classified (Soil Survey Staff, 1994) as Lithic Xerorthent (summit), Vertic Xerochrept (mid-slope), and Typic Pelloxerert (base). Mean annual temperature in the area is 16.7°C, mean annual rainfall is 521 mm

Copyright © 1999, The Clay Minerals Society

https://doi.org/10.1346/CCMN.1999.0470413 Published online by Cambridge University Press

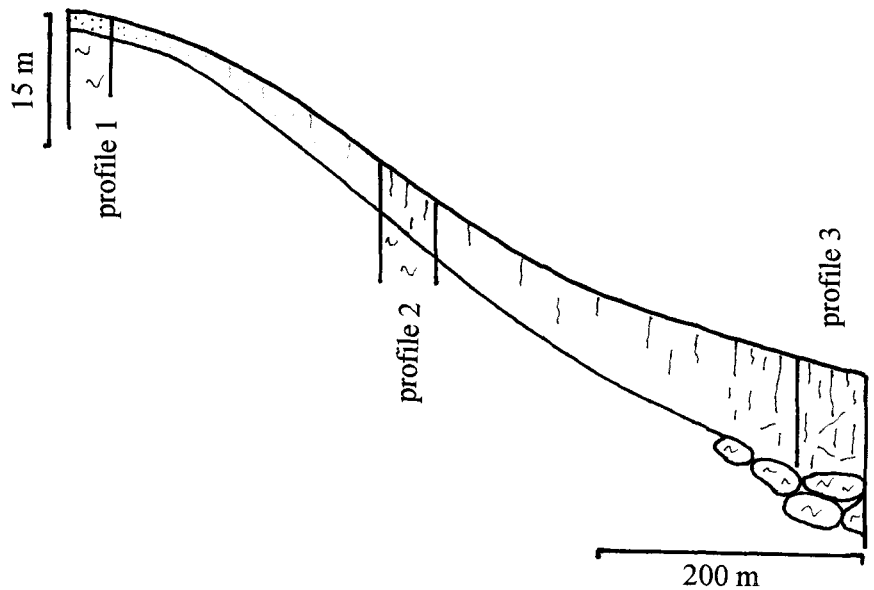

Figure 1. Schematic representation of the soil toposequence with location of the studied soils (soil profiles not to scale).

and potential evapotranspiration is 808 mm (Aru *et al.*, 1991). Climatic conditions may be described as thermic temperature and xeric water regimes. A short description of the three soil profiles is given in Table 1a with some analytical data (Table 1b).

Methods

The bulk soil samples were analyzed using SISS (Società Italiana Scienza del Suelo, 1985) methods: particle size analysis involved the pipette method, cation exchange capacity (CEC) was determined by $BaCl_2$ at pH 7, and exchangeable cations were determined by atomic absorption spectrometry (AAS).

Fine silt (2–5 μm) and clay (<2 μm) fractions were obtained from the soil horizons by sedimentation after removal of organic matter with dilute H_2O_2 buffered with Na-acetate. Amorphous and/or crystalline iron oxides and hydroxides were extracted with the dithionite-citrate-bicarbonate (DCB) treatment (Mehra and Jackson, 1960). A NaOH solution at pH 9 was used for dispersion. No treatment for dissolution of calcium carbonate was used to avoid possible alteration of clay minerals induced by acidification. The fine clay fraction (<0.1 μm) was obtained from the clay (<2 μm) fraction using a Beckman J2-21 centrifuge and a JCF-Z continuous flow rotor.

X-ray diffraction (XRD) patterns were obtained from oriented clay mineral aggregate specimens using a Philips diffractometer with Fe-filtered CoKα radiation. Pretreatment of the specimens included Ca saturation and solvation with ethylene glycol. The diffractograms were recorded using a DACO-MP recorder associated with a microcomputer using the Diffrac AT software (SOCABIM). The XRD patterns were then decomposed into their elementary component curves using an X-ray decomposition program (DECOMPXR, Lanson, 1993). Such decomposition is believed to improve the measure of the position and relative intensity of the diffraction peaks. The NEWMOD program (Reynolds, 1985) was used to simulate XRD patterns and to identify and quantify the K-S mixed layers.

Evaluation of the layer charge of the 2:1 expandable layers was made by expansion with alkylammonium ions following Olis *et al.* (1990). Alkylammonium ions in the interlayer may adopt either a monolayer (1.36 nm), a double layer (1.77 nm), or a pseudotrilayer (2.17 nm) configuration depending on the magnitude of the layer charge. For smectites and low-charge vermiculites, the layer charge may not be homogeneous; charge can vary between layers. Varying 2:1 layer charge results in an interstratification of the monolayer and bilayer (or the bilayer and pseudotrilayer) complexes, leading to non-integral *d*-values between 1.36–1.77 nm (or 1.77–2.17 nm) in XRD patterns. The mean layer charge is determined by the relative proportions of bilayers to monolayers (or pseudotrilayers to bilayers) as indicated from peak migration curve analysis of interstratified spacings. Thus, Olis *et al.* (1990) proposed an empirical method to determine the mean layer charge from *d*-values obtained after expansion with a single long chain alkylammonium (nC = 12). To apply this method to the expandable component in K-S mixed layers, the *d*(001)-values were determined for three-component mixed layers of bilayer (1.77 nm) and monolayer (1.36 nm) complexes (or pseudotrilayer, 21.7 nm, and bilayer complexes) in fixed proportions and kaolinite layers in proportions observed in the K-S samples (see be-

https://doi.org/10.1346/CCMN.1999.0470413 Published online by Cambridge University Press

Table 1a. Description of the three soil profiles.

Horizon thickness (cm)	Description and comments
	Summit (slope 0%): Profile 1
0–10: A[1]	Loam, very dark gray (10YR 3/1 moist), very friable, moderate fine and medium granular structure, coarse fragments <2–5%, no HCl effervescence, common fine and medium roots, linear abrupt boundary.
>10: R	Coherent weathered basaltic rock (fissures, dissolution features).
	Mid-Slope (slope 35%): Profile 2
0–10: A	Loam, very dark gray (10YR 3/1 moist), very friable, moderate fine, medium granular, and medium subangular blocky structure, coarse fragments 2–5%, no HCl effervescence, common fine and medium roots, linear clear boundary.
10–30: Bw	Loam, black (10YR 2/1), friable, fine and medium angular and subangular blocky structure, coarse fragments 5–15%, no HCl effervescence, common fine and few medium roots, undulate abrupt boundary.
>30: R	Coherent weathered basaltic rock (fissures, dissolution features).
	Footslope (Base, slope 1%): Profile 3
0–25: Ap	Clay loam, very dark gray (10YR 3/1 moist), friable, moderate fine granular and fine to coarse subangular blocky structure in the upper half, moderate to strong medium subangular blocky structure in the lower half, coarse fragments 2–5%, no HCl effervescence, common fine and medium roots, linear clear boundary.
25–50: Bss	Silty clay, black (10YR 2/1 moist), hard when dry, firm when moist, moderate to strong medium and coarse subangular blocky structure, slickensides, large cracks (5 mm width), coarse fragments 2–5%, slight HCl effervescence, few medium roots, linear gradual boundary.
50–80: Bss/C	Silty clay, black (10YR 2/1 moist), very hard when dry, very firm when moist, medium and coarse angular blocky structure, large peds have slickensides, coarse fragments <1%, slight HCl effervescence, few medium and fine roots.
>80: C	Continuous layer of large (20–50 cm) rounded blocks of basaltic rocks.

[1] See Soil Survey Staff (1994) for standard soil definitions.

low). The d(001)-values were determined using the NEWMOD program (Reynolds, 1985) for three-component systems. Empirical curves of mean layer charge *vs.* d(001)-values were then constructed for K-S mixed layers with 30 or 70% kaolinite layers (Figure 2).

The effect of Hofmann and Klemen (1950), which involves altering the octahedral charge in dioctahedral smectites by Li-saturation and heating at 300°C (Li-treatment), was used to distinguish octahedral from tetrahedral charges. Fine-clay CEC was measured by the procedure of Anderson and Sposito (1991) which distinguishes between accessible structural permanent charge and variable charge. The procedure was used before and after Li-treatment of the fine-clay fraction. The reduction of the CEC after Li-treatment was assumed to represent octahedral charge.

Total surface area of the fine clay was measured using the ethylene glycol monoethyl ether (EGME) technique (Heilman *et al.*, 1965). Fourier transform infrared (FTIR) spectroscopy was performed on KBr disks prepared by mixing 1 mg fine-clay with 300 mg KBr and pressing at 13 kg cm^{-2}. FTIR spectra were recorded using a Nicolet 510 spectrometer. Chemical analyses were performed on the fine clay following Jeanroy (1972): the samples were melted at 1100°C with Sr metaborate in an induction furnace, followed by dissolution of the glass pearl in diluted HCl. Atomic absorption spectrometry was used to analyze for Si, Al, Fe, Ti, Mg, Ca, Na, and K.

RESULTS

Soil analysis

The clay content (Table 1) in soil horizons increases from profile 1 (23.4%, A) to profile 3 (34.5%, Ap; 45.2%, Bss). Soil pH in H_2O increases from slightly acidic (5.7, A) for profile 1, to neutral (6.8, A; 6.6, Bw) for profile 2, to basic (8.7, Bss) in profile 3. The CEC of soil samples increases from 19.6 cmolc kg^{-1} for profile 1 (A horizon) to 28.0 cmolc kg^{-1} in the Ap and 31.4 cmolc kg^{-1} in the Bss horizon of profile 3. The proportion of K^+ and Ca^{2+} on the exchange sites decreases whereas Mg^{2+} increases from the top to the base of the soil toposequence. XRD patterns (not shown) of the silt fraction (5–20 μm) from the A and Bw horizons of profile 2 exhibit diffraction peaks of quartz (0.426 and 0.334 nm), feldspars, and pyroxenes (0.402, 0.375, 0.363, 0.319, 0.321, and 0.295 nm). No phyllosilicates are present in these samples.

XRD for fine-clay fraction

Profile 1. The XRD pattern of the fine-clay fraction (ethylene glycol solvated) from the shallow A horizon (Figure 3) indicates small amounts of kaolinite (peaks at 0.731 and 0.358 nm) and mica or illite (1.012 nm) together with clear features of a K-S mixed-layer mineral: diffraction peaks between 0.731–1.012 nm and 0.358–0.335 nm. The decomposition of the XRD pattern in the 8–16 and 27–33 °2θ regions (Figure 3) gives four derived curves in each region: the peak at 1.014 nm and at 0.334 nm is attributed to illite or mica; the peak at 0.906 nm and at 0.334 nm is attri-

https://doi.org/10.1346/CCMN.1999.0470413 Published online by Cambridge University Press

Table 1b. Characteristics of the soil horizons.

	Depth cm	Clay (<2 μm)	OM	pH (H_2O)	CEC	Na %CEC	K %CEC	Ca %CEC	Mg %CEC
Profile 1									
A	0–10	23.4	7.8	5.7	19.6	3.4	11.7	65.5	19.3
Profile 2									
A	0–10	25.9	4.0	6.8	19.3	3.5	3.3	54.7	38.4
Bw	10–30	31.0	2.2	6.6	22.5	2.9	1.9	51.7	43.5
Profile 3									
Ap	0–25	34.5	1.5	7.3	28.0	4.9	1.3	53.9	39.8
Bss	25–50	45.2	0.9	8.7	31.4	12.5	0.7	42.9	44.0

Clay (<2 μm), OM (organic matter): percent 105°C dry soil. CEC: $cmol_c\ kg^{-1}$. Na, K, Ca, Mg: exchangeable cations.

buted to illite-smectite mixed layers (I-S); the peak at 0.795 nm and at 0.343 nm is attributed to K-S mixed layers with (based on simulated XRD patterns) 70% kaolinite layers; the peak at 0.735 nm and at 0.355 and 0.358 nm is related to pure kaolinite or K-S mixed layers with <10% of expandable layers.

Profile 2. The XRD patterns of the fine-clay fraction from the A and Bw horizons are very similar and indicate K-S mixed layers as the dominant clay mineral (Figure 4). For the two fine-clay samples, the decomposition of the XRD patterns in the 8–16 °2θ region (Figure 5) gives three derived curves with maxima at 0.884, 0.795, and 0.738 nm. In the 27–33 °2θ region, three main derived curves are also obtained with maxima at 0.353, 0.343, and 0.334 nm (Figure 5). For profile 1, the peak at 0.884 nm and at 0.334 nm is attributed to I-S mixed layers, the peak at 0.795 nm associated with that at 0.343 nm is attributed to K-S mixed layers with 70% kaolinite layers and the peak at 0.738 nm and at 0.353 nm is related to K-S mixed layers with <10% expandable layers. An additional weak peak at 0.358 nm indicates small amounts of pure kaolinite.

Localization of the layer charge, either in the octahedral or tetrahedral sheet, was determined using the

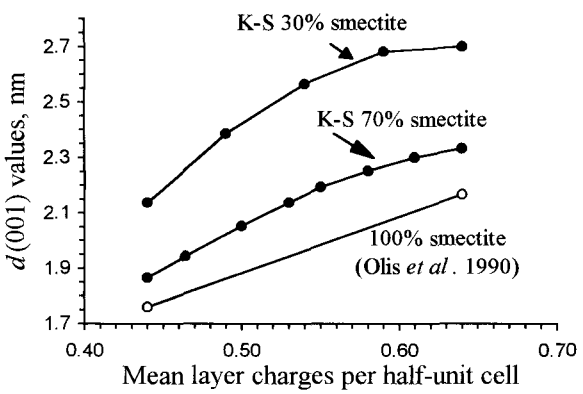

Figure 2. Mean layer charges *vs.* *d*(001)-values of dodecylammonium ion (*n*C = 12)-exchanged K-S mixed layers with 30 and 70% smectite layers.

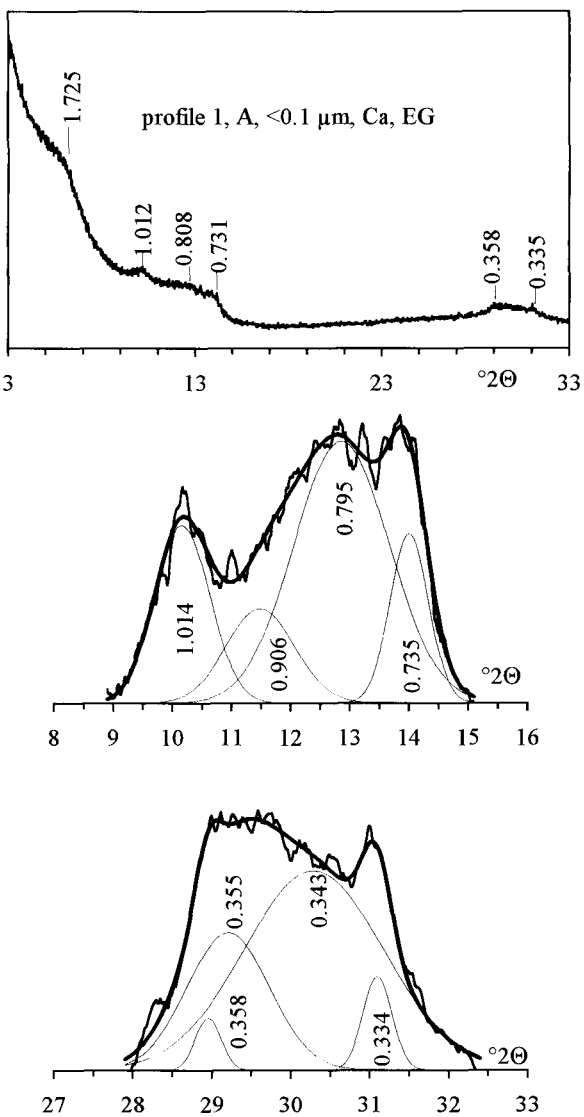

Figure 3. XRD pattern of the fine clay from profile 1 (EG: ethylene glycol solvated) and decomposition of the pattern in the 8–16 and 27–33 °2θ region. *d*-values in nm. CoKα radiation.

https://doi.org/10.1346/CCMN.1999.0470413 Published online by Cambridge University Press

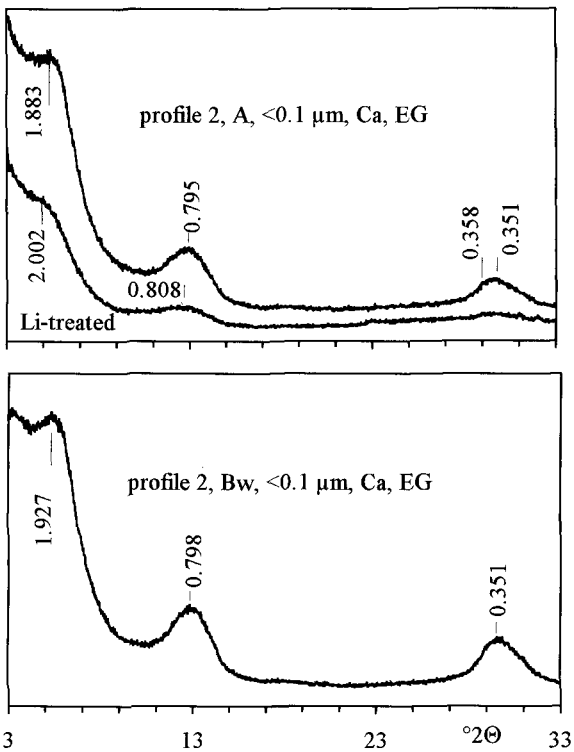

Figure 4. XRD patterns of the fine clay from profile 2, A and Bw horizons (EG: ethylene glycol solvated). Li-treated: Li-saturated and heated sample (Hofmann and Klemen effect). *d*-values in nm. CoKα radiation.

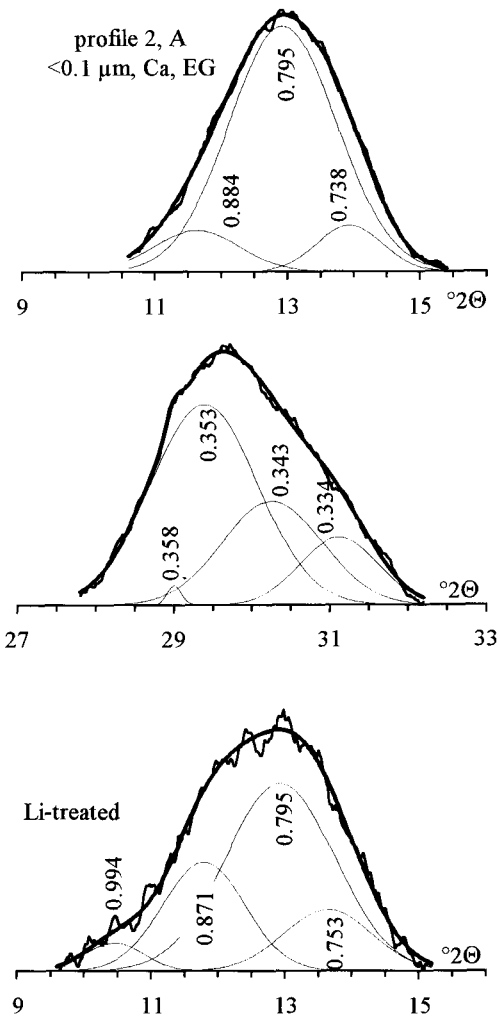

Figure 5. Decomposition of the XRD patterns of the fine clay from profile 2 (A horizon) in the 8–16 and 27–33 °2θ region. Li-treated: Li-saturated and heated sample (Hofmann and Klemen effect). *d*-values in nm. CoKα radiation.

Hofmann and Klemen effect (Li-treatment). After Li-treatment and ethylene glycol solvation, the XRD patterns for the fine clay from the A and Bw horizons remain almost unchanged (Figure 4). Only a small broadening of the peak near 1.88 nm is observed, indicating that a small proportion of smectite (montmorillonitic) layers are irreversibly collapsed. The decomposition of the XRD patterns of the Li-treated fine clays shows derived curves with maxima at 0.994, 0.871, 0.795, and 0.753 nm (Figure 5). Compared to the untreated fine clays, the maximum at 0.795 nm is unchanged, indicating that some of the K-S mixed layers have an expandable component that is beidellitic (re-expansion after Li-treatment). The other maxima have higher *d*-values than in the untreated fine clays, indicating that 0.97-nm layers (montmorillonitic layers) were formed during treatment. Thus the montmorillonitic layers are also a component of the K-S mixed layers. As noted by Moore and Reynolds (1997, p. 285), the formation of 0.97 nm spacings from 1.70 nm layers of smectite following heating or Li-treatment, increases the *d*-value of the composite diffraction peak of the K-S mixed-layer phase because the new composite diffraction peak combines the 001 peak of the dehydrated smectite (0.97 nm) instead of the 002 peak of the ethylene glycol preparation (0.86 nm). An estimate of the proportion of beidellitic to montmorillonitic layers in these samples is not possible because of the low number of smectite layers.

After intercalation of alkylammonium ions (*n*C = 12), the XRD pattern exhibits a large and poorly defined reflection with a maximum intensity at 2.44 nm (Figure 6), which indicates interstratification of bilayer and pseudotrilayer complexes. According to the calibration curve (Figure 2), a mean layer charge of 0.50 per half-unit cell occurs for the smectite component of the K-S mixed layers.

Profile 3. As for profile 2, the XRD patterns of the fine-clay fraction (ethylene glycol solvated) from the Ap and Bss horizons are very similar (Figure 7), indicating K-S mixed layers (peaks at 1.77, 0.563, and 0.842 nm) and small amounts of kaolinite (peaks at

https://doi.org/10.1346/CCMN.1999.0470413 Published online by Cambridge University Press

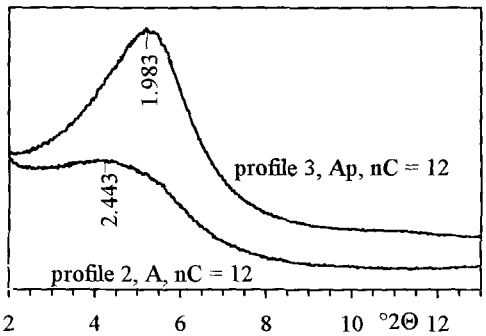

Figure 6. XRD patterns of dodecylammonium (nC = 12)-exchanged fine clay from A and Ap horizons of profile 2 and 3. d-values in nm. CoKα radiation.

0.718 and 0.358 nm). Decomposition of the XRD patterns in the 8–16 and 27–33 °2θ region gives two main derived curves with maxima at 0.842 and 0.746, and 0.353 and 0.339 nm, respectively (Figure 8). The peak at 0.842 nm and at 0.339 nm is attributed to K-S mixed layers with 30% kaolinite layers, the peak at 0.746 and at 0.353 nm is attributed to K-S mixed layers with <10% smectite layers. The derived curves with their maximum at 0.718 and 0.358 nm are attributed to pure kaolinite.

Following Li-treatment, the XRD patterns are greatly changed (Figure 7): the intensity of the 001 peak is decreased greatly and the position of the peak at 0.842 nm (untreated sample) shifted to higher d-values (0.878 nm). The decomposition of the XRD pattern from the Li-treated sample in the 8–16 °2θ region (not shown) gives four derived curves with maxima at 0.999, 0.881, 0.839, and 0.765 nm. Compared to the untreated sample, the position of all the elementary curves has shifted to higher d-values, indicating that 0.97-nm (montmorillonitic) layers were formed. A close simulation of the experimental pattern was obtained by computing three-component mixed layers with 30% kaolinite, 40% beidellitic smectite layers (expanded), and 30% montmorillonitic smectite layers (collapsed) (Figure 7). After intercalation with alkylammonium ions (nC = 12) the XRD pattern exhibits a large diffraction peak at 1.983 nm (Figure 6) indicating interstratification of bilayer and pseudotrilayer complexes and, based on Figure 2, a mean layer charge of 0.48 per half-unit cell for the smectite component in the K-S mixed layers.

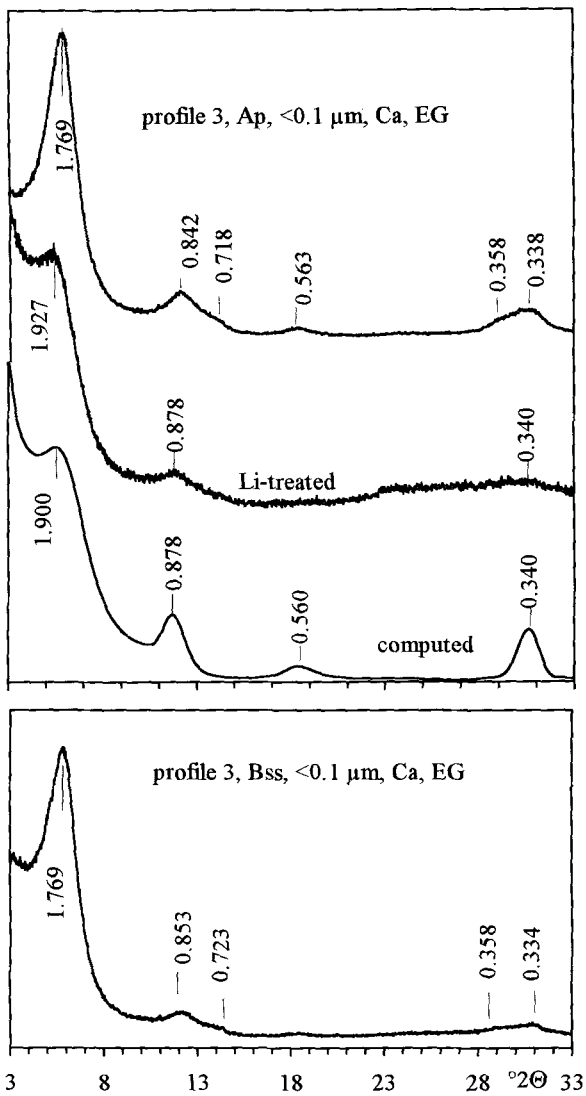

Figure 7. XRD patterns of the fine clay from profile 3, Ap and Bss horizons (EG: ethylene glycol solvated). Li-treated: Li-saturated and heated sample (Hofmann and Klemen effect). Computed: simulation of the XRD pattern of the Li-treated sample using NEWMOD program; random interstratification of 30% kaolinite, 40% expanded smectite (beidellite), and 30% collapsed smectite (montmorillonite) was used. d-values in nm. CoKα radiation.

Surface area and CEC measurements

The total surface areas (EGME method, Table 2) for the fine clay from profiles 2 and 3 are very similar for the two horizons in the same profile and larger for profile 3 (456–467 $m^2\ g^{-1}$) than for profile 2 (350–358 $m^2\ g^{-1}$). These results are in good agreement with XRD data showing more smectite layers in profile 3. Following Li-treatment, the total surface area is reduced to 285–297 $m^2\ g^{-1}$ for the fine clay of profile 2 and 350 $m^2\ g^{-1}$ for the fine clay of profile 3 (Table 2). The reduction is attributed to irreversible collapse of the montmorillonitic interlayers. Therefore, assuming that the external surface area was not modified by Li-treatment, the difference in areas before and after Li-treatment represents the internal surface of these layers. This surface is 65–61 $m^2\ g^{-1}$ (19–17% of the total surface area) in profile 2 and 106–117 $m^2\ g^{-1}$ (24–25% of the total surface area) in profile 3 (Table 2).

https://doi.org/10.1346/CCMN.1999.0470413 Published online by Cambridge University Press

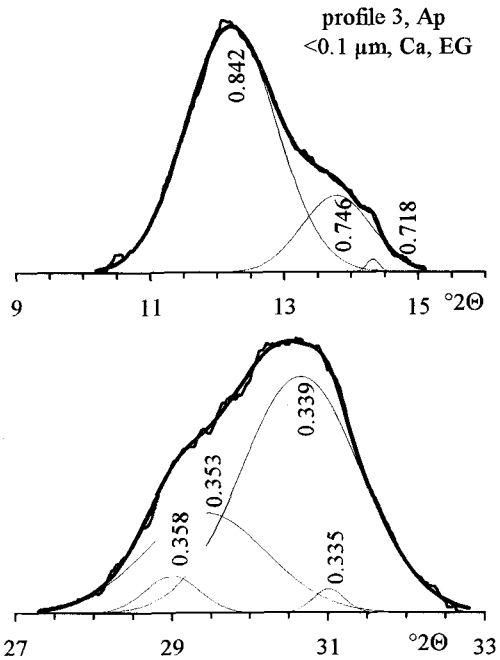

Figure 8. Decomposition of the XRD patterns of the fine clay from profile 3 (Ap horizon) in the 8–16 and 27–33 °2θ region. CoKα radiation. *d*-values in nm.

Thus, about the same proportion of montmorillonitic layers occurs in the fine clays from profile 2 and 3.

CEC for the fine clay increases from profile 1 (48.9 $cmol_c\ kg^{-1}$) to profile 2 (54.6 $cmol_c\ kg^{-1}$, A; 55.5 $cmol_c\ kg^{-1}$, Bw), and 3 (70.5 $cmol_c\ kg^{-1}$, Ap; 69.0 $cmol_c\ kg^{-1}$, Bss) (Table 3). For the five samples the contribution of the variable charge to the total CEC is quite similar and accounts for 15.2–16.8 $cmol_c\ kg^{-1}$. The accessible permanent charge located in the tetrahedral sheet was obtained from the fine clay of profiles 2 and 3 subjected to the Li-treatment (Table 3). This permanent charge of the tetrahedral sheet represents 64–67% and 69–70% of the total permanent charge for the fine clay of profiles 2 and 3, respectively. Thus, assuming that the origin of the permanent charge occurs in the smectite layers only, the distribution of the permanent (structural) charge between the tetrahedral and the octahedral sheet is very similar for the smectite component of the K-S mixed layers (with different proportion of smectite layers) from the two profiles. Moreover, a good correlation was found between the accessible permanent charge and the total surface area, both for the untreated and Li-treated fine-clay samples (Figure 9); this suggests that the mean surface charge density is very similar for all the smectite layers present in the different K-S mixed layers.

Table 2. Surface areas ($m^2\ g^{-1}$) for the fine clay fraction of studied horizons.

Horizon	TS	Li-TS	ΔTS	ΔTS %TS
Profile 2				
A	350	285	65	19
Bw	358	297	61	17
Profile 3				
Ap	456	350	106	23
Bss	467	350	117	25

TS: total surface area (EGME method).
Li-TS: total surface area of Li-treated samples.
ΔTS: TS-[Li-TS] (internal surface of montmorillonitic smectite layers).

Table 3. Cation exchange capacities ($cmol_c\ kg^{-1}$) of the fine clay fraction of studied horizons.

Horizon	CEC	APC	VC	Li-CEC	Li-APC	Li-APC %APC
Profile 1						
A	48.9	32.9	16.0	nd	nd	
Profile 2						
A	54.6	39.0	15.6	36.2	24.9	64
Bw	55.5	40.3	15.2	38.5	27.1	67
Profile 3						
Ap	70.5	53.8	16.7	49.9	38.3	70
Bss	69.0	52.1	16.9	49.4	36.1	69

APC: accessible permanent charge; VC: variable charge; CEC = APC + VC.
Li-CEC: CEC of Li-treated samples.
Li-APC: APC of Li-treated samples = accessible tetrahedral charge.
nd: not analyzed.

Fine clay-fraction analyses

Chemical analysis shows a gradual change in the chemical composition of the fine clay from profile 1 to profile 3 (Table 4). The K_2O contents are between 1.94% (profile 1) and 0.75–0.77% (profile 3), indicating that profile 1 has <20% of illite or mica layers and profile 3 has <8%, as no K-feldspars are present

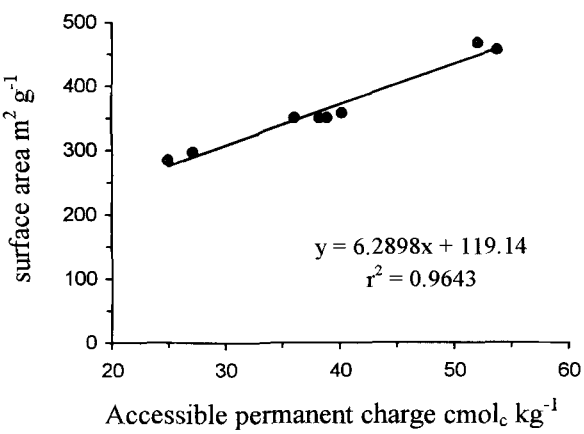

Figure 9. Accessible permanent charges *vs.* total surface areas for the fine clay of profiles 2 and 3 (A, Bw, Ap, and Bss horizons) including untreated and Li-treated samples.

https://doi.org/10.1346/CCMN.1999.0470413 Published online by Cambridge University Press

Table 4. Total analyses of the fine clay fraction of studied horizons as percent of 105°C dry sample.

Horizon	SiO_2	Al_2O_3	Fe_2O_3	MnO	MgO	CaO	Na_2O	K_2O	TiO_2	LOI
Profile 1										
A	45.10	22.89	9.75	0.02	1.34	0.42	0.98	1.94	0.97	16.90
Profile 2										
A	45.19	23.30	11.49	0.02	1.01	0.31	0.74	1.02	0.83	16.40
Bw	44.95	23.35	11.66	0.02	1.01	0.44	0.73	1.06	0.85	16.70
Profile 3										
Ap	45.24	18.31	12.70	0.03	2.01	0.42	0.78	0.77	1.19	18.70
Bss	45.20	18.38	13.53	0.03	2.54	0.42	1.18	0.75	1.36	16.90

LOI: loss on ignition.

in the samples. The MgO content is higher in profile 3, in good agreement with more smectite layers occurring in this profile. Because DCB treatment was used to remove iron oxides, Fe_2O_3 content is assumed to represent iron in the silicate; iron increases from profile 1 (9.75%) to profile 3 (12.7–13.53%) suggesting that it is located in the smectite and not the kaolinite layers.

FTIR spectroscopy

FTIR spectra are very similar for all the fine clays from the three profiles (Figure 10). High frequency IR bands occur at 3700 and 3625 cm^{-1} and these bands are characteristic for kaolinite. A distinct shoulder at 3600 cm^{-1} is also observed. This band is commonly assigned to OH-stretching vibrations of the $AlOHFe^{3+}$ groups in both smectites and Fe-rich kaolinite (Petit and Decarreau, 1990). In the present case, because Fe occurs mostly in the smectite, this band was assigned to $\nu AlOHFe^{3+}$ in smectite. For the OH-bending vibration region, two absorption bands are observed at 880 and 912 cm^{-1}. The former is assigned to $\delta AlOHFe^{3+}$ vibrations in smectites, for the same reason as given above. The latter at 912 cm^{-1} is commonly attributed to δAlOHAl vibrations in either kaolin minerals or Al-rich smectites. In this study, this band is attributed to kaolinite because no clear band of νAlOHAl in smectite was observed at ~3640 cm^{-1}. Comparison between the spectra from profiles 2 and 3 clearly shows that the relative intensity of the band due to kaolinite is higher for the fine clay of profile 2 than for that of profile 3, in good agreement with more kaolinite layers in profile 2. Moreover, because the spectra from the two profiles are qualitatively similar, no marked change in chemical composition of the smectite is observed.

DISCUSSION

The soil toposequence developed from basaltic rock which does not contain phyllosilicates (no biotite was found in the silt fraction from profile 2). Therefore, clay minerals in the soils are neogenic clays produced by weathering of minerals in the basaltic rock. There was no or very limited contamination by allochtoneous

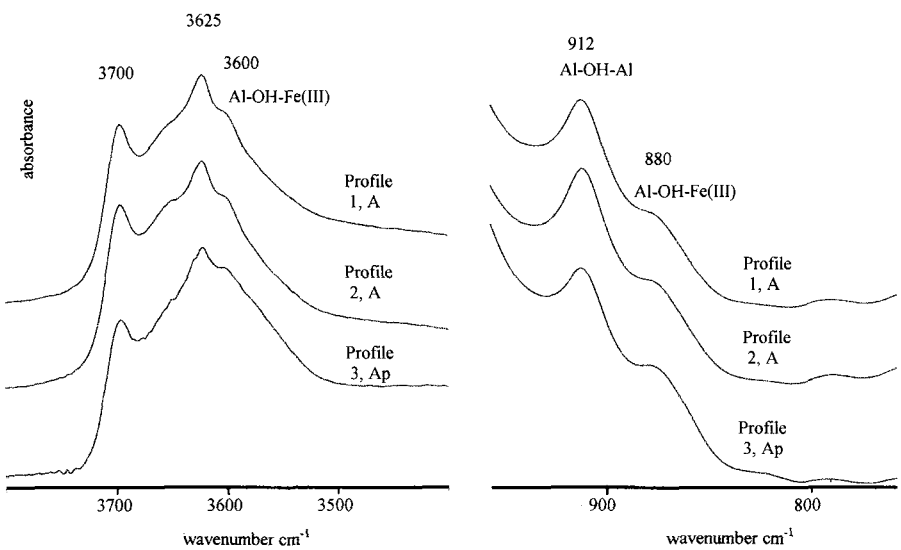

Figure 10. FTIR spectra of the fine clay from profile 1, 2, and 3 (A or Ap horizons).

https://doi.org/10.1346/CCMN.1999.0470413 Published online by Cambridge University Press

material at the base of the hill (profile 3), because no mica occurs in the silt fractions (not shown), although mica-bearing rocks (Miocene marls) are present in this area. Thus, the soil clay minerals are assumed to be derived from the pedogenic alteration of one basaltic parent material over the toposequence. However, translocation of fine clays from the top to the lower part of the slope can not be excluded. The small amount of K-S mixed layers with a high proportion of kaolinite layers (90%), which are present in profile 3, may possibly be attributed to clay minerals formed in the upper slope and translocated downslope.

K-S mixed layers in the studied soils were identified with increasing proportion of smectite layers downslope. This soil-clay mineral distribution, in relation to topography, is similar to that reported for (kaolinitic) red-black (smectitic) soil association in subtropical areas (Herbillon *et al.*, 1981; Kantor and Schwertmann, 1974). Drainage conditions induced by the slope gradient are thought to govern the soil clay mineralogical evolution. The steep slope promotes rapid downward movement of water, which removes silica and soluble cations (which favor the formation of kaolinite clay). Slopes with less grade have slower water-flow conditions, leading to more extensive water-rock interactions and higher silica and divalent cation concentrations in the soil solution. Thus the formation of smectite clay is favored (Velde, 1992). K-S mixed layers probably form wherever conditions of "intermediate" drainage occur. Our results suggest that the proportion of kaolinite in the K-S mixed-layer phase is related to drainage conditions also: the better the drainage, the greater the proportion of kaolinite layers. CEC and surface area reduction after Li-treatment was found to be very similar for all the K-S mixed layers, indicating that the smectite component is identical (same charge magnitude, distribution, and heterogeneity) along the toposequence. Also the chemical composition was found to be very similar along the toposequence based on FTIR spectroscopy.

A K-S mixed-layer phase occurred as the dominant clay mineral in the soil horizons of the three profiles. No thick saprolite is present in any of the studied soils. However, clay minerals were certainly produced in the weathered basaltic parent material. Fe-bearing smectites (nontronite, Fe-beidellite) are common products of basic rocks or basalt weathering (Ildefonse, 1987; Wilson, 1987), and they are usually confined to the lower portions of soil profiles. Therefore, initial weathering of the basaltic rock to produce a heterogeneous interstratification of smectite clay at the soil-bedrock weathering front is highly likely.

Hughes *et al.* (1993) discussed the mechanism of formation of K-S mixed layers, which remains poorly understood. A possible mechanism is the solid-state transformation of pre-existing smectite layers by "stripping away" the tetrahedral sheet. However, it is not clear if the tetrahedral charge would become neutralized before the sheet decomposes. Conversely, dissolution-recrystallization processes were proposed, where smectite and kaolinite layers crystallize directly from solution in response to oscillating chemical conditions in the microenvironment. Srodon (1980) suggested that K-S mixed-layer phases form because there is dissolution of some pre-existing smectite layers with subsequent crystallization of kaolinite in the interlayer region between smectite layers.

The smectite component of the K-S mixed layers studied here maintains the same structural characteristics regardless of the proportion of kaolinite layers present. It is unlikely that crystallization from soil solutions with different chemical chemistries has produced K-S mixed layers with the same heterogeneous smectite component. The mechanism by which one tetrahedral sheet of some smectite layers is removed to produce kaolinite layers allows the remaining smectite layers to maintain the magnitude and heterogeneous character of their layer charge, assuming there is no major alteration of the charge before the removal of the tetrahedral sheet. However, surviving tetrahedral sheets in the newly formed 1:1 layer would retain Al or Fe substitutions. This was not possible to establish with the data obtained. The fact that the chemical composition and layer charge of the smectite component are the same for K-S mixed-layer phases with various proportion of smectite layers is best explained by the mechanism of Srodon (1980): dissolution of some smectite layers with subsequent crystallization of kaolinite in the interlayer region of other smectite crystallites.

CONCLUSION

Pedogenic K-S mixed layer phases were formed in a soil toposequence developed from basaltic parent material under temperate climate with alternating wet and dry seasons. A fast internal drainage induced by a steep slope appears to be the major factor responsible for their formation. Drainage conditions probably affect the proportion of kaolinite in the K-S mixed-layer phases. As noted by previous investigators, the formation of K-S mixed-layer phases is an intermediate step in the transformation of smectite to kaolinite. The process involves removal of the tetrahedral sheet which, for the studied clays, would occur without previous alteration of the smectite-layer charge. More likely, complete dissolution of some smectite layers and crystallization of kaolinite occurs in the interlayers of the remaining smectite.

ACKNOWLEDGMENTS

This study was part of a cooperative program supported by CNR (Italy) and CNRS (France): Programme de Recherche en Coopération sur Conventions Internationales du CNRS, Projet #3187/1997. The authors would like to thank A. Aru,

https://doi.org/10.1346/CCMN.1999.0470413 Published online by Cambridge University Press

P. Baldaccini, and their collaborators for their essential support in choosing and sampling the study site.

REFERENCES

Anderson, S.J. and Sposito, G. (1991) Cesium-adsorption method for measuring accessible structural surface charge. *Soil Science Society of America Journal*, **55,** 1569–1576.

Aru, A., Baldacini, P., and Vacca, A. (1991) *Nota illustrativa alla carta dei suoli della Sardegna. Cagliari, Italia.* Regione Autonoma della Sardegnia and Universitâ degli studi di Cagliari, 83 pp.

Heilman, M.D., Carter, D.L., and Gonzalez, C.L. (1965) The ethylene glycol monoethyl ether (EGME) technique for determining soil-surface area. *Soil Science*, **100,** 409–413.

Herbillon, A.J., Frankart, R., and Vielvoye, L. (1981) An occurrence of interstratified kaolinite-smectite minerals in a red-black soil toposequence. *Clay Minerals*, **16,** 195–201.

Hofmann, V.U. and Klemen, R. (1950) Verlust der austauschfähigkeit von lithium-ionen an bentonit durch erhitzung. *Zeitung für Anorganische Chemie*, **262,** 95–99.

Hughes, R.E., Moore, D.M., and Reynolds, R.C., Jr. (1993) The nature, detection and occurrence, and origin of kaolinite/smectite. In *Kaolin Genesis and Utilization*, H.H. Murray, W.M. Bund, and C.C. Harvey, eds., Special Publication No 1, Clay Minerals Society, Boulder, Colorado, 291–323.

Ildefonse, P. (1987) Analyse pétrographique des altérations prémétéoriques et météoriques de deux roches basaltiques (basaltes de Belbex, Cantal et Hawaiite de M'Bouda, Cameroun). Doctoral thesis, Université de Paris 7, Paris, 142 pp.

Jaynes, W.F., Bigham, J.M., Smeck, N.E., and Shipitalo, M.J. (1989) Interstratified 1:1–2:1 mineral formation in a polygenetic soil from southern Ohio. *Soil Science Society of America Journal*, **53,** 1888–1894.

Jeanroy, E. (1972) Analyse totale des silicates naturels par spectrométrie d'absorption atomique. Application au sol et à ses constituants. *Chimie Analytique*, **54,** 159–166.

Kantor, W. and Schwertmann, U. (1974) Mineralogy and genesis of clays in red-black toposequences in Kenya. *Journal of Soil Science*, **25,** 67–78.

Lanson, B. (1993) *DECOMPXR, X-ray Decomposition Program.* ERM, Poitiers, France.

Mehra, O.P. and Jackson, M.L. (1960) Iron oxide removal from soils and clays by a dithionite-citrate system buffered with sodium bicarbonate. *Clays and Clay Minerals*, **7,** 317–327.

Moore, D.M. and Reynolds, R.C., Jr. (1997) *X-ray Diffraction and the Identification and Analysis of Clay Minerals, 2nd edition.* Oxford University Press, Oxford, 371 pp.

Olis, A.C., Malla, P.B., and Douglas, L.A. (1990) The rapid estimation of the layer charges of 2:1 expanding clays from a single alkylammonium ion expansion. *Clay Minerals*, **25,** 39–50.

Petit, S. and Decarreau, A. (1990) Hydrothermal (200°C) synthesis and crystal chemistry of iron-rich kaolinites. *Clay Minerals*, **25,** 181–196.

Reynolds, R.C. (1985) *NEWMOD a Computer Program for the Calculation of One-dimensional Diffraction Powders of Mixed-layer Clays.* R.C. Reynolds, 8 Brook Rd., Hanover, New Hampshire 03755 USA, 315 pp.

SISS (Società Italiana Scienza del Suelo). (1985) *Metodi normalizzati di analisi del suelo.* Edagricole, Bologna, 159 pp.

Soil Survey Staff. (1994) *Keys to Soil Taxonomy, 5th edition.* Pocahontas Press Blackburg, Virginia.

Srodon, J. (1980) Synthesis of mixed-layer kaolinite/smectite. *Clays Clay Minerals*, **28,** 419–424.

Velde, B. (1992) *Introduction to Clay Minerals. Chemistry, Origins, Uses and Environmental Significance.* Chapman & Hall, London, 198 pp.

Wilson, M.J. (1987) Soil smectites and related interstratified minerals: Recent developments. In *Proceedings of the International Clay Conference, Denver*, Bloomington, Indiana, L.G. Schultz, H. van Olphen, and F.A. Mupton, eds. The Clay Minerals Society, 167–173.

Wilson, M.J. and Cradwick, P.D. (1972) Occurrence of interstratified kaolinite-montmorillonite in some Scottish soils. *Clay Minerals*, **9,** 435–437.

Yerima, B.P.K., Calhoun, F.G., Senkayi, A.L., and Dixon, J.B. (1985) Occurrence of interstratified kaolinite-smectite in El Salvador Vertisols. *Soil Science Society of America Journal*, **49,** 462–466.

(Received 22 January 1998; accepted 28 February 1999; Ms. 98-014)

https://doi.org/10.1346/CCMN.1999.0470413 Published online by Cambridge University Press